

---

# Detecting multiple change-points in the time-varying Ising model

---

Batiste Le Bars<sup>†\*</sup>Pierre Humbert<sup>†</sup>Argyris Kalogeratos<sup>†</sup>Nicolas Vayatis<sup>†</sup>

<sup>†</sup>CMLA, CNRS, ENS Paris-Saclay,  
 Université Paris-Saclay,  
 94235, Cachan cedex, France.

<sup>\*</sup>Sigfox R&D  
 31670, Labège, France

## Abstract

This work focuses on the estimation of change-points in a time-varying Ising graphical model (outputs  $-1$  or  $1$ ) evolving in a piecewise constant fashion. The occurring changes alter the graphical structure of the model, a structure which we also estimate in the present paper. For this purpose, we propose a new optimization program consisting in the minimization of a penalized negative conditional log-likelihood. The objective of the penalization is twofold: it imposes the learned graphs to be sparse and, thanks to a fused-type penalty, it enforces them to evolve piecewise constantly. Using few assumptions, we then give a change-point consistency theorem. Up to our knowledge, we are the first to present such theoretical result in the context of time-varying Ising model. Finally, experimental results on several synthetic examples and a real-world dataset demonstrate the empirical performance of our method.

## 1 Introduction

Graphs are fundamental tools for revealing and studying static or varying relationships between variables of potentially high-dimensional vector-data. In the static scenario, the task of learning relationships between variables is referred as *graph inference* and emerges in many fields such as in Graph Signal Processing (Dong et al., 2016; Le Bars et al., 2019) or in physics and biology (Rodriguez et al., 2011; Du et al., 2012). In this work, we consider a probabilistic framework where the

observed data are drawn from an *Ising model*, which is a discrete *Markov Random Field* (MRF) with  $\{-1, 1\}$ -outputs. MRF are undirected probabilistic graphical models (Koller et al., 2009) where a set of random variables are represented as different nodes of a graph. In this graph an edge between two nodes indicates that the two corresponding random variables are dependent given the other variables.

Using a set of observations to estimate the structure of such probabilistic graphical models has been widely investigated (Banerjee et al., 2008). In particular for Gaussian Graphical Models (GGM) (Meinshausen et al., 2006; Yuan and Lin, 2007; Ren et al., 2015) with the graphical lasso (Friedman et al., 2008). Learning the parameters of an Ising model is also addressed by several papers in the literature (Guo et al., 2010; Höfling and Tibshirani, 2009; Ravikumar et al., 2010; Xue et al., 2012).

Over the past years, however, there has been a burst of interest in investigating variations and changes occurring over time in real-world networks. Take for example the brain functional activity network that radically changes during an epilepsy (Kramer et al., 2008) or faced to an external stimuli such as anesthesia. Similar observations can be made for several network cases, namely social, transportation, communication, or biological networks (e.g. interacting genes (Friedman et al., 2008)).

Thus, the interest on the problem of *change-point detection* emerges naturally for time-varying probabilistic graphical models that are of particular significance for studying dynamic phenomena. In fact, this has been extensively investigated in time-varying MRFs with piecewise constant structure. The Gaussian case has been particularly explored (Wang et al., 2018), either algorithmically (Hallac et al., 2017; Gibberd and Nelson, 2017), or theoretically (Kolar and Xing, 2012) for all the possible variations of the change-point detection problem: single (Bybee and Atchadé, 2018) or multiple (Gibberd and Roy, 2017) change-points;

---

Part of this work was funded by the IdAML Chair hosted at ENS Paris-Saclay.

offline (Kolar and Xing, 2012) or online (Keshavarz et al., 2018) detection, etc.

Notably, the advancements related to the time-varying Ising model are a lot more limited. In Ahmed and Xing (2009) and Kolar et al. (2010), the authors introduce the task of fitting the parameters of a time-varying Ising model without emphasis on the change-point detection problem, and without providing a theoretical understanding of their approach. Only the single change-point detection method in Roy et al. (2017) comes with theoretical analysis.

**Contribution.** In this work we consider the task of detecting an unknown number of change-points in a time-varying Ising model with piecewise constant parameters, while also being able to estimate the varying graph structure. In technical terms we introduce an optimization program using a fused-type penalty (Harchaoui and Lévy-Leduc, 2010; Kolar and Xing, 2012). Contrarily to Ahmed and Xing (2009) and Kolar et al. (2010), we propose the use of the  $\ell_2$ -norm as fused penalty, which allows us to derive a consistency theorem for the detected change-points. To the best of our knowledge, we are the first to provide such a theoretical result. The proposed method is referred as **TVI-FL**, which stands for Time-Varying Ising model identified with Fused and Lasso penalties.

The paper is organized as follows. First, we briefly recall important properties of the static Ising model and describe its piecewise constant version. Second, we present our methodology to infer the piecewise constant graph structure over time and the timestamps at which abrupt changes occur. Then, we present our main theoretical result which consist in a change-point detection consistency theorem. Finally, results on simulated data show empirically that our method outperforms the Gaussian version of it (Kolar and Xing, 2012), so as the method based on a  $\ell_1$  total-variation penalty (Ahmed and Xing, 2009), with respect to our simulation process. An additional real-world experiment done on a telecommunication dataset shows promising results.

## 2 The time-varying Ising model

Let us first recall that the *static Ising model* is a discrete MRF with  $\{-1, 1\}$ -outputs. This model is defined by a graph  $G = (V, E)$  and is associated to a symmetric weight matrix  $\Omega \in \mathbb{R}^{p \times p}$  whose non-zero elements correspond to the set of edges  $E$ . Formally, for the the  $(a, b)$ -th element of  $\Omega$  is  $\omega_{ab} \neq 0$  iff  $(a, b) \in E$ . An Ising model is thus entirely described by its associated weight matrix  $\Omega$ . Let  $X \sim \mathcal{I}(\Omega)$  be a random vector following an Ising model, with realizations

$x \in \{-1, 1\}^p$ , then its associated probability function is given by:

$$\mathbb{P}_\Omega(X = x) = \frac{1}{Z(\Omega)} \exp \left\{ \sum_{a < b} x_a x_b \omega_{ab} \right\}, \quad (1)$$

where  $Z(\Omega) = \sum_{x \in \{-1, 1\}^p} \exp \left\{ \sum_{a < b} x_a x_b \omega_{ab} \right\}$  is the the normalizing constant, and  $x_a, x_b$  are respectively the  $a$ -th and  $b$ -th coordinates of  $x$ . In the following we write  $\mathbb{P}_\Omega(X = x) = \mathbb{P}_\Omega(x)$ .

Due to the intractability of the normalizing constant  $Z$ , most Ising model inference methods use the conditional probability distribution function of a node  $a \in V$  knowing the other nodes  $V \setminus a$  given by:

$$\mathbb{P}_{\omega_{a\cdot}}(x_a | x_{\setminus a}) = \frac{\exp \left\{ 2x_a \sum_{b \in V \setminus a} x_b \omega_{ab} \right\}}{\exp \left\{ 2x_a \sum_{b \in V \setminus a} x_b \omega_{ab} \right\} + 1}, \quad (2)$$

where  $\omega_{a\cdot}$  denotes the  $a$ -th column (or row) of  $\Omega$  that is used to parametrize the probability function of Eq. (2). Here,  $x_{\setminus a}$  denotes the vector  $x$  without the coordinate  $a$ .

A *time-varying Ising model* is defined by a set of  $n$  graphs  $G_i = (V, E_i)$ ,  $i \in \{1, \dots, n\}$  over a fixed set of nodes  $V$  through a time-varying set of edges  $\{E_i\}_{i=1}^n$ . Like in the static case, each  $G_i$  is associated to a symmetric weight matrix  $\Omega^{(i)} \in \mathbb{R}^{p \times p}$  and an independent distribution  $\mathbb{P}_{\Omega^{(i)}}$  given by Eq. (1). A random variable associated to this model is a set of  $n$  independent random vectors  $X^{(i)} \sim \mathcal{I}(\Omega^{(i)})$ , hence a single realization is a set of  $n$  vectors, each denoted by  $x^{(i)} \in \{-1, 1\}^p$ .

In addition, we assume that the model is *piecewise constant*, i.e. there exist a collection of timestamps  $\mathcal{D} \triangleq \{T_1, \dots, T_D\} \subset \{2, \dots, n\}$ , sorted in ascending order, and a set of real-valued symmetric matrices  $\{\Theta^j\}_{j=1}^D$  such that  $\forall i \in \{1, \dots, n\}$ :

$$\Omega^{(i)} = \sum_{j=0}^D \Theta^{j+1} \mathbb{1}(T_j \leq i < T_{j+1}), \quad (3)$$

with  $T_0 = 1$  and  $T_{D+1} = n + 1$ , while  $D$  is the number of change-points considered by the model. According to Eq. (3), for a fixed  $j \in \{0, \dots, D\}$ , the set  $\{x^{(i)} : T_j \leq i < T_{j+1}\}$  contains iid vector samples drawn from  $\mathbb{P}_{\Theta^{j+1}}$ .

## 3 Learning Methodology

Assuming the observation of a single realization  $\{x^{(i)}\}_{i=1}^n$  of the described time-varying model, our objective is twofold. Firstly, we want to recover the set of change-points  $\mathcal{D}$ , and secondly, we want to recover the graph structure underlying the observed data vectors,

i.e. which edges are activated at each time-stamp. We next describe our methodology to perform those tasks.

Due to the complexity of our model and the aforementioned intractability of the normalizing constant  $Z(\cdot)$ , classical maximum likelihood approaches are difficult to apply. Hence, we extend the neighborhood selection strategy introduced for the static setting of Ravikumar et al. (2010) to our time-varying setting. Instead of maximizing the global likelihood of Eq. (1), this approach maximizes, for each node, the conditional likelihood of the node knowing the other nodes. As in the Gaussian version of our framework (Kolar and Xing, 2012), the proposed **TVI-FL** method, uses a fused-like penalty to infer the change-points and assumes that for each submodel the underlying graph is sparse. With such approach, at each timestamp, the local neighborhood of each node is selected with a penalized logistic regression method given in the next section.

### 3.1 Optimization program

For each node  $a = 1, \dots, p$ , we solve the program:

$$\hat{\beta}_a = \underset{\beta \in \mathbb{R}^{p-1 \times n}}{\operatorname{argmin}} \mathcal{L}_a(\beta) + \operatorname{pen}_{\lambda_1, \lambda_2}(\beta), \quad (4)$$

where  $\mathcal{L}_a(\beta)$  stands for the negative conditional log-likelihood of the node  $a$ , knowing the rest of the nodes. It has a closed-form given by:

$$\mathcal{L}_a(\beta) \triangleq - \sum_{i=1}^n \log \left( \mathbb{P}_{\beta^{(i)}}(x_a^{(i)} | x_{\setminus a}^{(i)}) \right) \quad (5)$$

$$\begin{aligned} &= \sum_{i=1}^n \log \left\{ \exp \left( \beta^{(i)T} x_{\setminus a}^{(i)} \right) + \exp \left( -\beta^{(i)T} x_{\setminus a}^{(i)} \right) \right\} \\ &\quad - \sum_{i=1}^n x_a^{(i)} \beta^{(i)T} x_{\setminus a}^{(i)}, \end{aligned} \quad (6)$$

where  $\beta^{(i)}$  stands for the  $i$ -th column of  $\beta$ . The last row is obtained by plugging Eq. (2) in Eq. (5) with  $\beta^{(i)}$  instead of  $\omega_a$ .

Provided two positive hyperparameters,  $\lambda_1$  and  $\lambda_2$ , the penalty function  $\operatorname{pen}_{\lambda_1, \lambda_2}(\beta)$  that we propose to take is the following:

$$\operatorname{pen}_{\lambda_1, \lambda_2}(\beta) = \lambda_1 \sum_{i=2}^n \|\beta^{(i)} - \beta^{(i-1)}\|_2 + \lambda_2 \sum_{i=1}^n \|\beta^{(i)}\|_1.$$

With such an objective function, we learn at each timestamp  $i$  the neighborhood of the node  $a$  given by the  $i$ -th column of  $\beta$ . The penalty function is necessary to prevent overfitting. In particular, without the first term, we would fit for each timestamp  $i \in \{1, \dots, n\}$  a parameter vector  $\beta^{(i)}$  that perfectly matches the observation  $x^{(i)}$  (in terms of likelihood). In such situation,

we would obtain as many different parameter vectors  $\beta$  as the different samples, making the piecewise constant assumption (Eq. 3) impossible to get. On the contrary here, the  $\ell_2$ -norm encourages consecutive parameter vectors to be equal. The second term, also important to prevent overfitting, especially when the number of nodes is big, allows the learned parameter vectors to be sparse and thus imposes structure in the learned graphs. Knowing that, the hyperparameter  $\lambda_1$  controls the number of estimated change-points – the bigger  $\lambda_1$  is, the lower the number of estimated change-points is. Similarly, when  $\lambda_2$  increases, the sparsity of each parameter vector increases as well.

### 3.2 Change-point detection and structure identification

Now assume that the optimization program (4) is completed. The set of estimated change-points  $\hat{D}$  is:

$$\hat{D} = \left\{ \hat{T}_j \in \{2, \dots, n\} : \|\hat{\beta}_a^{\hat{T}_j} - \hat{\beta}_a^{\hat{T}_j-1}\|_2 \neq 0 \right\},$$

namely the set of timestamps at which the estimated parameter vectors have changed. The total number of estimated change-points is given by the cardinality of  $\hat{D}$ , let that be  $\hat{D} = |\hat{D}|$ .

If we are interested in learning the graph weights for each submodel  $j = 1, \dots, \hat{D} + 1$ , the  $a$ -th column of  $\Theta^j$  is estimated by  $\hat{\theta}_a^j = \hat{\beta}_a^{\hat{T}_j-1} = \dots = \hat{\beta}_a^{\hat{T}_j-1}$ . All the non-zero elements of  $\hat{\theta}_a^j$  indicate the *neighborhood* of  $a$ .

One should notice that this estimation would lead to a non-symmetric weight matrix (directed graphs). To face this problem, the authors of Ravikumar et al. (2010); Kolar and Xing (2012) propose to either use the min or max operator. For example, to estimate the structure of the  $j$ -th graph, we take:

$$\hat{E}_j = \{(a, b) : \max(|\hat{\theta}_{ab}^j|, |\hat{\theta}_{ba}^j|) > 0\},$$

where  $\hat{\theta}_{ab}^j$  is the  $b$ -th element of  $\hat{\theta}_a^j$  and conversely for  $\hat{\theta}_{ba}^j$ . In this case, there is an edge between two nodes if at least one of the nodes  $a$  and  $b$  contains the other node in its neighborhood.

## 4 Theoretical analysis

In this section, we present a change-point consistency theorem when the right number of change-points is estimated. This property states that when the number of samples tends to infinity, the time instances at which the change-points occur are well-estimated. Although left for future work, this consistency result is fundamental to obtain the consistency of the estimated graph structures, as it is the case in former works in

time-varying Gaussian graphical models (Kolar and Xing, 2012; Gibberd and Roy, 2017).

#### 4.1 Assumptions

We now give two important quantities in order to introduce the main assumptions of our theorem. Denoting by  $[D]$  the set of indices  $\{1, \dots, D\}$ , the first quantity is the minimal time difference between two change-points and is given by:

$$\Delta_{\min} \triangleq \min_{j \in [D]} |T_j - T_{j-1}|.$$

The second one is the minimal variation in parameters between two change-points and is given by:

$$\xi_{\min} \triangleq \min_{j \in [D]} \|\theta_a^{j+1} - \theta_a^j\|_2.$$

The following assumptions are assumed to be true for each node  $a \in V$ .

**(A1)** There exist two constants  $\phi_{\min} > 0$  and  $\phi_{\max} < \infty$  such that  $\forall j \in [D+1]$ ,  $\phi_{\min} \leq \Lambda_{\min} \left( \mathbb{E}_{\theta_a^j} [X_{\setminus a} X_{\setminus a}^T] \right)$  and  $\phi_{\max} \geq \Lambda_{\max} \left( \mathbb{E}_{\theta_a^j} [X_{\setminus a} X_{\setminus a}^T] \right)$ . Here  $\Lambda_{\min}$  and  $\Lambda_{\max}$  denote respectively the smallest and largest eigenvalues of the input matrix.

**(A2)** There exists a constant  $C > 0$  such that  $\max_{j, l \in [D+1]} \|\theta_a^j - \theta_a^l\|_2 \leq C$  and a constant  $M$  such that  $\max_{j \in [D+1]} \|\theta_a^j\|_2 \leq M$ .

**(A3)** The sequence  $\{T_j\}_{j=1}^D$  satisfies, for each  $j$ ,  $T_j = \lfloor n\tau_j \rfloor$ , where  $\{\tau_j\}_{j=1}^D$  is a fixed, unknown sequence of the change-point fractions belonging to  $[0, 1]$ . This allows to have enough samples in each of the submodels, as  $n$  goes to infinity.

#### 4.2 A change-point consistency theorem

In this section, we show *the change-point consistency* when the right number of change-points are estimated. The proof is made for a unique node  $a$  but generalizes to all the other nodes. We first give optimality conditions necessary to the global proof.

**Lemma 1.** (*Optimality Conditions*) *A matrix  $\hat{\beta}$  is optimal for problem (4) if and only if there exist a collection of subgradient vectors  $\{\hat{\mathbf{z}}_i\}_{i=2}^n$  and  $\{\hat{\mathbf{y}}_i\}_{i=1}^n$ , with  $\hat{\mathbf{z}}_i \in \partial \|\hat{\beta}^{(i)} - \hat{\beta}^{(i-1)}\|_2$  and  $\hat{\mathbf{y}}_i \in \partial \|\hat{\beta}^{(i)}\|_1$ , that for all  $k = 1, \dots, n$  they satisfy:*

$$\begin{aligned} & \sum_{i=k}^n x_{\setminus a}^{(i)} \left\{ \tanh \left( \hat{\beta}^{(i)T} x_{\setminus a}^{(i)} \right) - \tanh \left( \omega_a^{(i)T} x_{\setminus a}^{(i)} \right) \right\} \\ & - \sum_{i=k}^n x_{\setminus a}^{(i)} \left\{ x_{\setminus a}^{(i)} - \mathbb{E}_{\Omega^{(i)}} \left[ X_{\setminus a} | X_{\setminus a} = x_{\setminus a}^{(i)} \right] \right\} \\ & + \lambda_1 \hat{\mathbf{z}}_k + \lambda_2 \sum_{i=k}^n \hat{\mathbf{y}}_i = \mathbf{0}_{p-1}, \end{aligned} \quad (7)$$

$$\begin{aligned} & \text{with } \hat{\mathbf{z}}_1 = \mathbf{0}_{p-1}, \\ & \hat{\mathbf{z}}_i = \begin{cases} \frac{\hat{\beta}^{(i)} - \hat{\beta}^{(i-1)}}{\|\hat{\beta}^{(i)} - \hat{\beta}^{(i-1)}\|_2} & \text{if } \hat{\beta}^{(i)} - \hat{\beta}^{(i-1)} \neq \mathbf{0} \\ \in \mathcal{B}_2(0, 1) & \text{otherwise} \end{cases}, \\ & \hat{\mathbf{y}}_i = \begin{cases} \text{sign}(\hat{\beta}^{(i)}) & \text{if } x \neq 0 \\ \in \mathcal{B}_1(0, 1) & \text{otherwise} \end{cases} \\ & \text{and } \tanh \text{ the hyperbolic tangent function.} \end{aligned}$$

*Proof.* The proof is given in the Appendix. It consists in writing the sub-differential of the objective function and say, thanks to the convexity, that 0 belongs to it.  $\square$

**Theorem 1.** (*Change-point consistency*) *Let  $\{x_i\}_{i=1}^n$  be a sequence of observation drawn from a piecewise constant Ising model presented in Sec. 2. Suppose that the assumptions described earlier hold, and assume that  $\lambda_1 \asymp \lambda_2 = \mathcal{O}(\sqrt{\log(n)/n})$ . Let  $\{\delta_n\}_{n \geq 1}$  be a non-increasing sequence that converges to 0, and such that  $\forall n > 0$ ,  $\Delta_{\min} \geq n\delta_n$ , with  $n\delta_n \rightarrow +\infty$ . Assume further that (i)  $\frac{\lambda_1}{n\delta_n \xi_{\min}} \rightarrow 0$ , (ii)  $\frac{\sqrt{p-1}\lambda_2}{\xi_{\min}} \rightarrow 0$ , and (iii)  $\frac{\sqrt{p \log(n)}}{\xi_{\min} \sqrt{n\delta_n}} \rightarrow 0$ .*

*Then, if the right number of change-points are estimated ( $\hat{D} = D$ ), we have:*

$$\mathbb{P} \left( \max_{j=1, \dots, D} |\hat{T}_j - T_j| > n\delta_n \right) \rightarrow 0. \quad (8)$$

*Proof.* The proof closely follows the steps given in Harcaoui and Lévy-Leduc (2010); Kolar and Xing (2012); Gibberd and Roy (2017) which can be found in the Appendix. We present here a sketch of proof. First of all, thanks to the union bound, the probability of Eq. (8) can be upper bounded by:

$$\mathbb{P} \left( \max_{j=1, \dots, D} |\hat{T}_j - T_j| > n\delta_n \right) \leq \sum_{j=1}^D \mathbb{P}(|\hat{T}_j - T_j| > n\delta_n).$$

To prove Eq. (8), it is now sufficient to show  $\forall j = 1, \dots, D$  that  $\mathbb{P}(|\hat{T}_j - T_j| > n\delta_n) \rightarrow 0$ . Let us define the event  $C_n = \{|\hat{T}_j - T_j| < \frac{\Delta_{\min}}{2}\}$  and its complementary  $C_n^c$ . The rest of the proof is divided in two parts: bounding the good scenario, namely shows that  $\mathbb{P}(\{|\hat{T}_j - T_j| > n\delta_n\} \cap C_n) \rightarrow 0$  and doing the same for the bad scenario i.e  $\mathbb{P}(\{|\hat{T}_j - T_j| > n\delta_n\} \cap C_n^c) \rightarrow 0$ .

To show the first scenario, the proof applies Lemma 1 to bound the considered probability by three others probabilities. Those latter are then asymptotically bounded by 0 thanks to a combination of the Assumptions (A1-A3), the assumptions of the theorem and concentration inequalities related to the considered time-varying Ising model given in the lemmas of the Appendix.

To bound the bad case scenario, the three following complementary events are defined:

$$\begin{aligned} D_n^{(l)} &\triangleq \left\{ \exists j \in [D], \widehat{T}_j \leq T_{j-1} \right\} \cap C_n^c, \\ D_n^{(m)} &\triangleq \left\{ \forall j \in [D], T_{j-1} < \widehat{T}_j < T_{j+1} \right\} \cap C_n^c, \\ D_n^{(r)} &\triangleq \left\{ \exists j \in [D], \widehat{T}_j \geq T_{j+1} \right\} \cap C_n^c. \end{aligned}$$

Thus, it suffices to prove that  $\mathbb{P}(\{|\widehat{T}_j - T_j| > n\delta_n\} \cap D_n^{(l)})$ ,  $\mathbb{P}(\{|\widehat{T}_j - T_j| > n\delta_n\} \cap D_n^{(m)})$  and  $\mathbb{P}(\{|\widehat{T}_j - T_j| > n\delta_n\} \cap D_n^{(r)})$  tends to 0 as  $n$  goes to infinity. To prove this, similar arguments to those used for the good case are again employed.  $\square$

## 5 Simulated Experiments

### 5.1 Preliminary questions about the optimization procedure

The first question that rises is how to solve the program (4). Although non-differentiable, due to the convexity of the objective function there are several solvers available to minimize such a function. In our experiments, we use the python package CVXPY (Diamond and Boyd, 2016). Note that, since the optimization of each node parameter is independent, all these can be optimized in parallel.

Another technical remark about the optimization step is that, in some situations, the data vectors that we observe does not necessarily belong to  $\{-1, 1\}^p$  but to  $\{0, 1\}^p$  instead. In this case, the proposed method is essentially the same, except that the negative log-likelihood must be replaced by:

$$\sum_{i=1}^n \log \left\{ 1 + \exp \left( x_a^{(i)} \beta^{(i)T} x_a^{(i)} \right) \right\} - \sum_{i=1}^n x_a^{(i)} \beta^{(i)T} x_a^{(i)}.$$

In some cases, we may observe more than one data vector at each timestamp. Again, in this case, one has to replace the negative log-likelihood by the following:

$$-\sum_{i=1}^n \sum_{l=1}^{n_i} \log \left( \mathbb{P}_{\beta^{(i)}} \left( x_a^{(il)} | x_a^{(il)} \right) \right), \quad (9)$$

where  $n_i$  stands for the number of data vectors observed at timestamp  $i$  and  $x^{(il)}$  for the  $l$ -th observed vector at time  $i$ .

The last technical issue concerns the choice of the hyperparameters  $\lambda_1$  and  $\lambda_2$ . In Kolar and Xing (2012) and Ahmed and Xing (2009), the authors note that the problem of learning the weights actually corresponds to a supervised classification task. Indeed, our

optimization function actually corresponds to the regression of a node give the others as explanatory variables. For this reason they propose to either use cross-validation techniques or BIC for model selection. In this work we use the BIC, first used in Kolar et al. (2010), which consist in averaging for all nodes the following quantity:

$$\text{BIC}(\widehat{\beta}_a) \triangleq \mathcal{L}_a(\widehat{\beta}_a) - \frac{\log n}{2} \text{Dim}(\widehat{\beta}_a), \quad (10)$$

where

$$\begin{aligned} \text{Dim}(\widehat{\beta}_a) &= \sum_{i=2}^n \sum_{b \in V \setminus a} \mathbb{1}\{\text{sign}(\widehat{\beta}_{ab}^{(i)}) \neq \text{sign}(\widehat{\beta}_{ab}^{(i-1)})\} \\ &\quad \times \mathbb{1}\{\text{sign}(\widehat{\beta}_{ab}^{(i)}) \neq 0\}. \end{aligned}$$

We will see that, despite being easy to compute, BIC does not necessarily identify the best model regarding our learning tasks.

### 5.2 Experimental setup

**Baseline methods.** We compare our method, TVI-FL, to two state-of-the-art approaches. The first one, referred as TD-lasso (Kolar and Xing, 2012), corresponds to the Gaussian version of our algorithm. Indeed, it assumes that the output of the graphical models are Gaussian data and their proposed optimization program is the one of Eq. (4), where the negative likelihood function is replaced by  $\sum_{i=1}^n (x_a^{(i)} - \beta^{(i)T} x_a^{(i)})^2$ . The second approach, named TESLA (Ahmed and Xing, 2009), is closely related to our method as it simply replaces the  $\ell_2$ -norm in the penalty function by the  $\ell_1$ -norm. However, this method should not be seen as proper competitor. Indeed, as explained in (Hallac et al., 2017), the difference in using either the  $\ell_1$ - or the  $\ell_2$ -norm resides in the type of changes we aim to detect. The  $\ell_1$ -norm will be best-suited to the detection of local changes in the neighborhood of a node, whereas the  $\ell_2$ -norm will be more appropriate for the detection of global changes.

**Simulation design.** We propose to compare the methods' performance on 10 totally independent synthetic datasets. For each of them, the total number of time-instances is  $n = 100$  and number of change-points  $D = 2$ , resulting in 3 submodels. The 50 first time-instances are dedicated to the first submodel, the next 30 for the second, and the last 20 for the third one.

Then, for each of the 3 submodels, we generate independently a random regular graph of size  $p = 20$  with the degree of all nodes equal to  $d = 2, 3, 4, 5$ . To draw such random graph, we used the generator developed in the python package Networkx (Hagberg et al.,

Degree	Method	Precision	Recall	$F_1$ -score	$h$ -score
$d=2$	<b>TVI-FL</b>	<b>0.657</b> $\pm$ 0.119	0.892 $\pm$ 0.130	<b>0.754</b> $\pm$ 0.120	<b>0.065</b> $\pm$ 0.057
	Tesla	0.434 $\pm$ 0.131	0.641 $\pm$ 0.134	0.513 $\pm$ 0.129	0.167 $\pm$ 0.220
	TD-lasso	0.369 $\pm$ 0.064	<b>0.980</b> $\pm$ 0.014	0.534 $\pm$ 0.069	0.072 $\pm$ 0.055
$d=3$	<b>TVI-FL</b>	<b>0.628</b> $\pm$ 0.169	0.731 $\pm$ 0.132	<b>0.673</b> $\pm$ 0.151	<b>0.064</b> $\pm$ 0.070
	Tesla	0.289 $\pm$ 0.057	0.521 $\pm$ 0.120	0.365 $\pm$ 0.058	0.253 $\pm$ 0.245
	TD-lasso	0.437 $\pm$ 0.011	<b>0.963</b> $\pm$ 0.020	0.601 $\pm$ 0.013	0.090 $\pm$ 0.049
$d=4$	<b>TVI-FL</b>	0.338 $\pm$ 0.139	0.684 $\pm$ 0.180	0.421 $\pm$ 0.097	0.091 $\pm$ 0.116
	Tesla	0.313 $\pm$ 0.028	0.539 $\pm$ 0.077	0.394 $\pm$ 0.035	0.156 $\pm$ 0.225
	TD-lasso	<b>0.415</b> $\pm$ 0.055	<b>0.874</b> $\pm$ 0.034	<b>0.562</b> $\pm$ 0.056	<b>0.076</b> $\pm$ 0.071
$d=5$	<b>TVI-FL</b>	0.383 $\pm$ 0.130	0.665 $\pm$ 0.136	0.462 $\pm$ 0.070	0.076 $\pm$ 0.146
	Tesla	0.336 $\pm$ 0.033	0.454 $\pm$ 0.044	0.385 $\pm$ 0.030	0.155 $\pm$ 0.224
	TD-lasso	<b>0.411</b> $\pm$ 0.079	<b>0.773</b> $\pm$ 0.050	<b>0.534</b> $\pm$ 0.078	<b>0.064</b> $\pm$ 0.066

Table 1: Results obtained by selecting the model with the lowest BIC. The average and standard deviation of metrics are reported.

2008). Note also that, for a fixed example, the degree of the graph remains the same across the three submodels. The 10 experiments are actually performed for the four values of  $d$ , resulting in 40 experiments per dataset in total.

Now that we have the the graph structure of the Ising models, we need the edge weights. As in the paper of Ahmed and Xing (2009), for each edge, the corresponding weight is drawn from a uniform distribution taken over  $[-1, -0.5] \cup [0.5, 1]$ .

Finally we need to draw the observations following the corresponding submodel. To do so, we used Gibbs sampling with a burn-in period of 1000 samples and a lag of 20 between each sample to avoid dependency between the observation. Furthermore, to accelerate the convergence, we observe 10 (instead of just 1) vectors of size 20 at each time-instance. It results in the sample of  $100 \times 10$  observations for each of the 40 examples and in the use of the likelihood of Eq. (9).

**Performance metrics.** We use four different metrics usually used in such experiments. The first one, the Hausdorff metric ( $h$ -score), measures the performance of the estimated set of change-points  $\hat{\mathcal{D}}$ . It corresponds to the greatest temporal distance between a change-point and its prediction:

$$h(\mathcal{D}, \hat{\mathcal{D}}) \triangleq \frac{1}{n} \max \left\{ \max_{t \in \mathcal{D}} \min_{\hat{t} \in \hat{\mathcal{D}}} |t - \hat{t}|, \max_{\hat{t} \in \hat{\mathcal{D}}} \min_{t \in \mathcal{D}} |t - \hat{t}| \right\},$$

and has to be as small as possible.

The other metrics, namely *precision*, *recall*, and  $F_1$  score, concern the goodness of the learned graph struc-

ture. They are given by the following equations:

$$precision = \frac{1}{n} \sum_{i=1}^n \frac{\sum_{a=1b=a+1}^{p-1} \sum_{a=1b=a+1}^p \mathbb{1}\{(a, b) \in \hat{E}_i \wedge (a, b) \in E_i\}}{\sum_{a=1b=a+1}^{p-1} \sum_{a=1b=a+1}^p \mathbb{1}\{(a, b) \in \hat{E}_i\}},$$

$$recall = \frac{1}{n} \sum_{i=1}^n \frac{\sum_{a=1b=a+1}^{p-1} \sum_{a=1b=a+1}^p \mathbb{1}\{(a, b) \in \hat{E}_i \wedge (a, b) \in E_i\}}{\sum_{a=1b=a+1}^{p-1} \sum_{a=1b=a+1}^p \mathbb{1}\{(a, b) \in E_i\}},$$

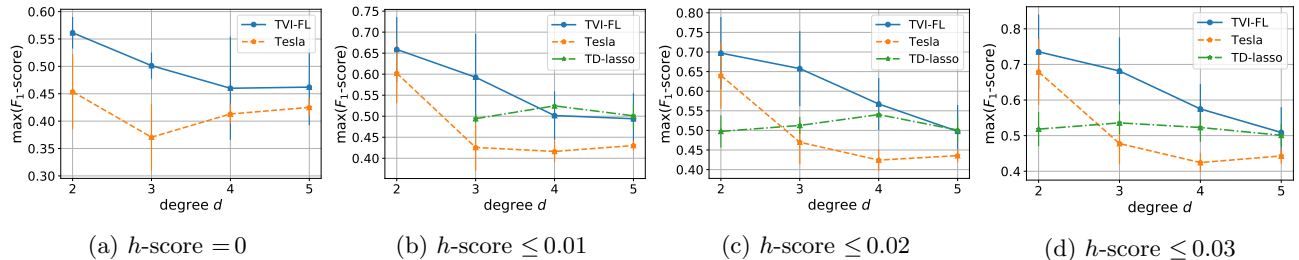
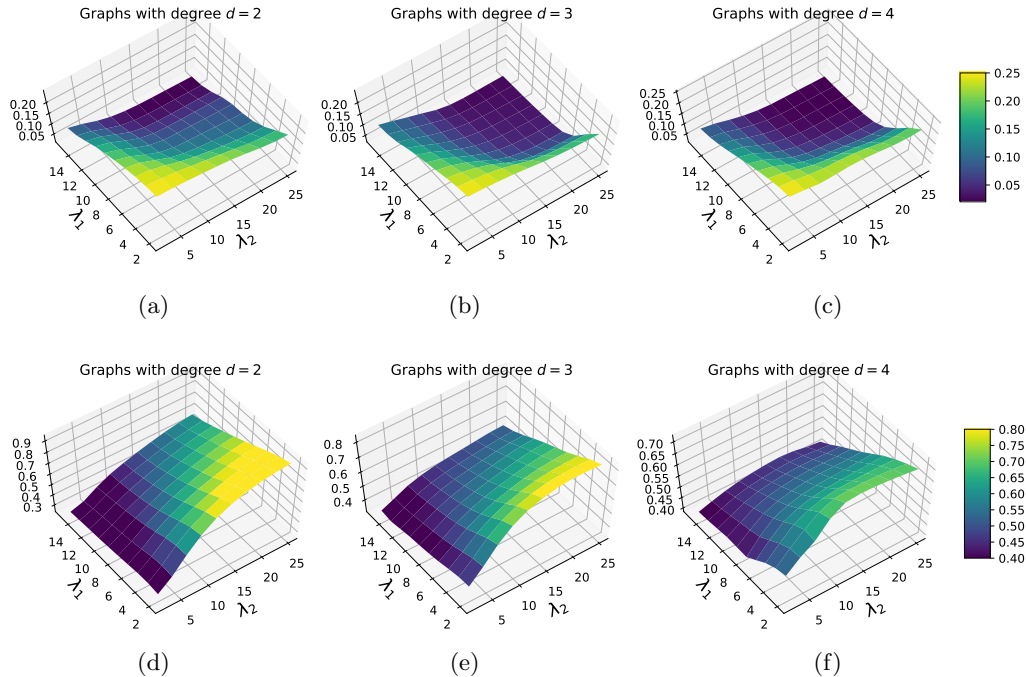
$$F_1 = \frac{2 \times precision \times recall}{precision + recall}.$$

A final remark concerns the choice of the two hyperparameters. We performed a grid-search strategy to find the best pair of values for  $(\lambda_1, \lambda_2)$  in  $[2, 15] \times [2, 25]$  for TVI-FL and TESLA, and  $(\lambda_1, \lambda_2)$  in  $[10, 25] \times [20, 40]$  for TD-lasso.

### 5.3 Results

To begin with, for each experiment and for each degree  $d$ , we select the models with the lowest BIC (Eq. (10)). Associated metrics are collected in Tab. 1. For  $d=2$  or 3, TVI-FL obtains the best results in terms of graph reconstruction and change-point detection, e.g. when  $d=2$  the average  $F_1$ -score and  $h$ -score are equal to 0.754 and 0.065, against 0.513 and 0.167 for Tesla, and 0.534 and 0.072 for TD-Lasso. On the contrary, when  $d$  increases, the BIC fails to select the best model for our method, which results in better performances for TD-Lasso.

In the following, we empirically prove that it is possible to obtain more accurate results on both  $h$ -score


 Figure 1: Average maximal value of the  $F_1$ -score for different  $h$ -score settings.

 Figure 2: Heat-maps of the average  $h$ -score (a)(b)(c) and  $F_1$ -score (b)(e)(f) obtained with TVI-FL when the degree of each node  $d$  is equal to 2, 3, or 4.

and  $F_1$ -score with a better selection of the hyperparameters. To do so, for each experiment and for each degree  $d$ , we select the model with the highest  $F_1$ -score when the associated  $h$ -score is: (a) equal to 0, or (b) lower than 0.01, or (c) 0.02, or (d) 0.03. In other words, we evaluate the best  $F_1$ -score when the worst change-point error is equal to 0 or lower than 1, 2 or 3 timestamps. The results are displayed in Fig. 1. First of all, it shows that for a lower  $h$ -score, TVI-FL is able to obtain similar  $F_1$ -score than those displayed in Tab. 1. Furthermore, we observe that it almost always gives better  $F_1$ -score than the competitors. Notice that, during our experiments, no model from TD-Lasso reached an  $h$ -score equal to 0.0, and hence it is not displayed in Fig. 1(a). In conclusion, although having similar results as the graph density increases, with a better model selection could help TVI-FL to outperform the state-of-the-art methods. In the Appendix,

we provide the table of results when the  $h$ -score is lower than 0.03. It confirms that BIC does not select the best set of hyperparameters, and that TVI-FL outperforms the competitors by selecting them properly.

Finally we display in Fig. 2 the heat-maps of the average  $h$ -score and  $F_1$ -score with respect to  $\lambda_1$  and  $\lambda_2$  when the degree of each node is  $d=2, 3$ , or 4. From these heat-maps, we see that when  $d=3$ , both  $\lambda_1$  and  $\lambda_2$  need to be high enough (greater than 10 and 20) to obtain a  $h$ -score lower than 0.03. On the contrary, to obtain an  $F_1$ -score greater than 0.75,  $\lambda_1$  need to be lower than 5 and  $\lambda_2$  greater than 14. Hence, there is a trade-off between accurately detecting the change-points (low  $h$ -score) and recovering accurately graph structure (high  $F_1$ -score). As an example, if we want  $h$ -score  $< 0.03$ , we need to set  $\lambda_1 > 10$  and  $\lambda_2 > 20$ , but with such values we cannot have  $F_1$ -score higher than 0.65. The same empirical conclusion can be made for

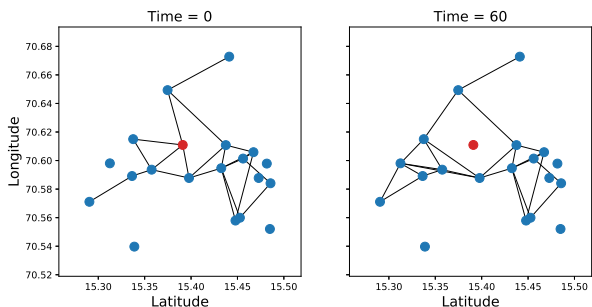


Figure 3: Learned graphs from the Sigfox dataset before and after the anomaly recorded at antenna shown in red.

the other node degrees. Heat-maps of the other methods are given in the Appendix and corroborate the idea of finding a trade-off. It appears that compared to them, the trade-off is easier to find for TVI-FL, as a wide range of  $\lambda_1, \lambda_2$  are suitable.

#### 5.4 A real-world example

In this section, we evaluate the goodness of graph learning with TVI-FL on the Sigfox IoT dataset (Le Bars and Kalogeratos, 2019). It consists in data from a telecommunication network, where each observation corresponds to a message that has been received by a subset of 34 antennas. Each data vector is binary and indicates which antennas has received the message or not (received = 1, not received = 0). The dataset contains all the messages received by the antennas, on a daily basis over a period of five months, resulting in  $n = 120$  timestamps. According to the authors, one antenna is working poorly after timestamp number 30. In the following experiment, we selected this antenna so as the 19 geographically closest others, and we selected randomly  $n_i = 200$  messages at each timestamp. The learned graphs with TVI-FL at timestamps  $i = 0$  (before the antenna problem) and  $i = 60$  (during the antenna problem) are displayed in Fig. 3 (only the positive edges are drawn).

The goodness-of-fit of our method can be corroborated by the two following observations; 1) The learned graphs are in adequacy with the spatial distribution of the antennas: nearby antennas are more likely to be connected. This was expected as nearby antennas have higher chance to receive the same messages, 2) The failing antenna lost edges between the two graphs. Again, this could have been expected since a poorly working antenna would receive less messages, implying a decreasing correlation with its neighbors.

## 6 Conclusion and future work

This paper proposed a new optimization program to learn a time-varying Ising model with piecewise constant structure. To the best of our knowledge, it is the first to provide a change-point consistency theorem and an empirical comparative study with the previous works on both time-varying Ising (Ahmed and Xing, 2009; Kolar et al., 2010) and Gaussian (Kolar and Xing, 2012) graphical models. Future directions of research include the investigation of a more adapted way to solve the optimization program, extensive real-world experiments, and improving the theoretical analysis with the proof of consistent graph structure estimation (*sparsistency*).

## References

- Ahmed, A. and Xing, E. P. (2009). Recovering time-varying networks of dependencies in social and biological studies. *Proc. of the National Academy of Sciences*, 106(29):11878–11883.
- Banerjee, O., Ghaoui, L. E., and dAspremont, A. (2008). Model selection through sparse maximum likelihood estimation for multivariate Gaussian or binary data. *J. of Machine Learning Research*, 9(Mar):485–516.
- Bybee, L. and Atchadé, Y. (2018). Change-point computation for large graphical models: a scalable algorithm for Gaussian graphical models with change-points. *J. of Machine Learning Research*, 19(1):440–477.
- Diamond, S. and Boyd, S. (2016). CVXPY: A Python-embedded modeling language for convex optimization. *J. of Machine Learning Research*, 17(83):1–5.
- Dong, X., Thanou, D., Frossard, P., and Vandergheynst, P. (2016). Learning Laplacian matrix in smooth graph signal representations. *Trans. Signal Processing*, 64(23):6160–6173.
- Du, N., Song, L., Yuan, M., and Smola, A. (2012). Learning networks of heterogeneous influence. In *Advances in Neural Information Processing Systems*, pages 2780–2788.
- Friedman, J., Hastie, T., and Tibshirani, R. (2008). Sparse inverse covariance estimation with the graphical lasso. *Biostatistics*, 9(3):432–441.
- Gibberd, A. J. and Nelson, J. D. (2017). Regularized estimation of piecewise constant Gaussian graphical models: The group-fused graphical lasso. *J. of Computational and Graphical Statistics*, 26(3):623–634.
- Gibberd, A. J. and Roy, S. (2017). Multiple changepoint estimation in high-dimensional Gaussian graphical models. *arXiv preprint arXiv:1712.05786*.
- Guo, J., Levina, E., Michailidis, G., and Zhu, J. (2010). Joint structure estimation for categorical Markov networks.
- Hagberg, A., Swart, P., and S Chult, D. (2008). Exploring network structure, dynamics, and function using networkx. Technical report.
- Hallac, D., Park, Y., Boyd, S., and Leskovec, J. (2017). Network inference via the time-varying graphical lasso.



- In *Proc. of the ACM SIGKDD Int. Conf. on Knowledge Discovery and Data Mining*, pages 205–213. ACM.
- Harchaoui, Z. and Lévy-Leduc, C. (2010). Multiple change-point estimation with a total variation penalty. *J. of the American Statistical Association*, 105(492):1480–1493.
- Höfling, H. and Tibshirani, R. (2009). Estimation of sparse binary pairwise Markov networks using pseudo-likelihoods. *J. of Machine Learning Research*, 10(Apr):883–906.
- Keshavarz, H., Michailidis, G., and Atchade, Y. (2018). Sequential change-point detection in high-dimensional Gaussian graphical models. *arXiv preprint arXiv:1806.07870*.
- Kolar, M., Song, L., Ahmed, A., Xing, E. P., et al. (2010). Estimating time-varying networks. *The Annals of Applied Statistics*, 4(1):94–123.
- Kolar, M. and Xing, E. P. (2012). Estimating networks with jumps. *Electronic Journal of Statistics*, 6:2069.
- Koller, D., Friedman, N., and Bach, F. (2009). *Probabilistic graphical models: principles and techniques*. MIT press.
- Kramer, M. A., Kolaczyk, E. D., and Kirsch, H. E. (2008). Emergent network topology at seizure onset in humans. *Epilepsy research*, 79(2-3):173–186.
- Le Bars, B., Humbert, P., Oudre, L., and Kalogeratos, A. (2019). Learning Laplacian matrix from bandlimited graph signals. In *IEEE Intern. Conf. on Acoustics, Speech and Signal Processing*, pages 2937–2941.
- Le Bars, B. and Kalogeratos, A. (2019). A probabilistic framework to node-level anomaly detection in communication networks. In *IEEE Conference on Computer Communications*, pages 2188–2196.
- Meinshausen, N., Bühlmann, P., et al. (2006). High-dimensional graphs and variable selection with the lasso. *The Annals of Statistics*, 34(3):1436–1462.
- Ravikumar, P., Wainwright, M. J., Lafferty, J. D., et al. (2010). High-dimensional ising model selection using  $\ell_1$ -regularized logistic regression. *The Annals of Statistics*, 38(3):1287–1319.
- Ren, Z., Sun, T., Zhang, C.-H., Zhou, H. H., et al. (2015). Asymptotic normality and optimalities in estimation of large Gaussian graphical models. *The Annals of Statistics*, 43(3):991–1026.
- Rodriguez, M., Balduzzi, D., and Schölkopf, B. (2011). Uncovering the temporal dynamics of diffusion networks. In *Proc. of the Int. Conf. on Machine Learning*, pages 561–568.
- Roy, S., Atchadé, Y., and Michailidis, G. (2017). Change point estimation in high dimensional Markov random-field models. *J. of the Royal Statistical Society: Series B (Statistical Methodology)*, 79(4):1187–1206.
- Wang, B., Qi, Y., et al. (2018). Fast and scalable learning of sparse changes in high-dimensional Gaussian graphical model structure. In *Int. Conf. on Artificial Intelligence and Statistics*, pages 1691–1700.
- Xue, L., Zou, H., Cai, T., et al. (2012). Nonconcave penalized composite conditional likelihood estimation of sparse ising models. *The Annals of Statistics*, 40(3):1403–1429.
- Yuan, M. and Lin, Y. (2007). Model selection and estimation in the Gaussian graphical model. *Biometrika*, 94(1):19–35.

## Supplementary material

### Technical proofs

**Lemma 1.** (*Optimality Conditions*) A matrix  $\hat{\beta}$  is optimal for problem (4) if and only if there exist a collection of subgradient vectors  $\{\hat{\mathbf{z}}_i\}_{i=2}^n$  and  $\{\hat{\mathbf{y}}_i\}_{i=1}^n$ , with  $\hat{\mathbf{z}}_i \in \partial \left\| \hat{\beta}^{(i)} - \hat{\beta}^{(i-1)} \right\|_2$  and  $\hat{\mathbf{y}}_i \in \partial \left\| \hat{\beta}^{(i)} \right\|_1$ , that satisfies for all  $k = 1, \dots, n$ :

$$\begin{aligned} & \sum_{i=k}^n x_a^{(i)} \left\{ \tanh \left( \hat{\beta}^{(i)T} x_a^{(i)} \right) - \tanh \left( \omega_a^{(i)T} x_a^{(i)} \right) \right\} \\ & - \sum_{i=k}^n x_a^{(i)} \left\{ x_a^{(i)} - \mathbb{E}_{\Omega^{(i)}} \left[ X_a | X_a = x_a^{(i)} \right] \right\} \\ & + \lambda_1 \hat{\mathbf{z}}_k + \lambda_2 \sum_{i=k}^n \hat{\mathbf{y}}_i = \mathbf{0}_{p-1} \end{aligned} \quad (1)$$

with  $\hat{\mathbf{z}}_1 = \mathbf{0}_{p-1}$ ,  

$$\hat{\mathbf{z}}_i = \begin{cases} \frac{\hat{\beta}^{(i)} - \hat{\beta}^{(i-1)}}{\left\| \hat{\beta}^{(i)} - \hat{\beta}^{(i-1)} \right\|_2} & \text{if } \hat{\beta}^{(i)} - \hat{\beta}^{(i-1)} \neq \mathbf{0} \\ \in \mathcal{B}_2(0, 1) & \text{otherwise} \end{cases},$$

$$\hat{\mathbf{y}}_i = \begin{cases} \text{sign}(\hat{\beta}^{(i)}) & \text{if } x \neq 0 \\ \in \mathcal{B}_1(0, 1) & \text{otherwise} \end{cases}$$
and  $\tanh$  the hyperbolic tangent function.

*Proof.* The proof follows those of Harchaoui and Lévy-Leduc (2010); Kolar and Xing (2012) and Gibberd and Roy (2017). We first introduce the following change of variables:

$$\gamma^{(i)} = \begin{cases} \beta^{(i)} & \text{if } i = 1 \\ \beta^{(i)} - \beta^{(i-1)} & \text{otherwise.} \end{cases}$$

Thus  $\beta^{(i)} = \sum_{l=1}^i \gamma^{(l)}$ , which leads to a change in the objective function (4) of the main paper:

$$\begin{aligned} \{\hat{\gamma}^{(i)}\}_{i=1}^n &= \underset{\gamma \in \mathbb{R}^{p-1 \times n}}{\operatorname{argmin}} \sum_{i=1}^n \log \left\{ \exp \left( \sum_{l=1}^i \gamma^{(l)T} x_a^{(i)} \right) \right. \\ & \quad \left. + \exp \left( - \sum_{l=1}^i \gamma^{(l)T} x_a^{(i)} \right) \right\} \\ & - \sum_{i=1}^n x_a^{(i)} \sum_{l=1}^i \gamma^{(l)T} x_a^{(i)} + \lambda_1 \sum_{i=2}^n \left\| \gamma^{(i)} \right\|_2 \\ & + \lambda_2 \sum_{i=1}^n \left\| \sum_{l=1}^i \gamma^{(l)} \right\|_1. \end{aligned} \quad (2)$$

This problem is convex, thus a necessary and sufficient condition for  $\{\hat{\gamma}^{(i)}\}_{i=1}^n$  to be a solution is that for all

$k = 1, \dots, n$ , the  $(p-1)$ -dimensional zero vector  $\mathbf{0}$ , belongs to the subdifferential of (2), taken with respect to  $\gamma^{(k)}$ :

$$\begin{aligned} \mathbf{0} \in & \sum_{i=k}^n x_a^{(i)} \left( \tanh \left( \sum_{l=1}^i \hat{\gamma}^{(l)T} x_a^{(i)} \right) - x_a^{(i)} \right) \\ & + \lambda_1 \partial \left\| \hat{\gamma}^{(k)} \right\|_2 + \lambda_2 \sum_{i=k}^n \partial \left\| \sum_{l=1}^i \hat{\gamma}^{(l)} \right\|_1. \end{aligned}$$

Recall that  $\partial \|x\|_2 = \begin{cases} \left\{ \frac{x}{\|x\|_2} \right\} & \text{if } x \neq 0 \\ \mathcal{B}_2(0, 1) & \text{otherwise} \end{cases}$  and  $\partial \|x\|_1 = \begin{cases} \{\text{sign}(x)\} & \text{if } x \neq 0 \\ \mathcal{B}_1(0, 1) & \text{otherwise} \end{cases}$ . Reapplying the change of variable, we obtain:

$$\mathbf{0} = \sum_{i=k}^n x_a^{(i)} \left( \tanh \left( \hat{\beta}^{(i)T} x_a^{(i)} \right) - x_a^{(i)} \right) + \lambda_1 \hat{\mathbf{z}}_k + \lambda_2 \sum_{i=k}^n \hat{\mathbf{y}}_i$$

Noting that  $\mathbb{E}_{\Omega^{(i)}} \left[ X_a | X_a = x_a^{(i)} \right] = \tanh \left( \omega_a^{(i)T} x_a^{(i)} \right)$ , we obtain the final result.  $\square$

**Theorem 1.** (*Change-point consistency*) Let  $\{x_i\}_{i=1}^n$  be a sequence of observation drawn from piece-wise constant Ising model presented in Section 2. Suppose that the assumptions described upper holds and assume that  $\lambda_1 \asymp \lambda_2 = \mathcal{O}(\sqrt{\log(n)/n})$ . Let  $\{\delta_n\}_{n \geq 1}$  be a non-increasing sequence that converges to 0 and such that  $\forall n > 0$ ,  $\Delta_{\min} \geq n\delta_n$ , with  $n\delta_n \rightarrow +\infty$ . Furthermore assume that  $\frac{\lambda_1}{n\delta_n \xi_{\min}} \rightarrow 0$  (i),  $\frac{\sqrt{p-1}\lambda_2}{\xi_{\min}}$  (ii) and  $\frac{\sqrt{p \log(n)}}{\xi_{\min} \sqrt{n\delta_n}} \rightarrow 0$  (iii). Then, if the right number of change-points are estimated ( $\hat{D} = D$ ), we have:

$$\mathbb{P} \left( \max_{j=1, \dots, D} |\hat{T}_j - T_j| > n\delta_n \right) \rightarrow 0. \quad (3)$$

*Proof.* The proof closely follows the steps given in Harchaoui and Lévy-Leduc (2010); Kolar and Xing (2012); Gibberd and Roy (2017). First of all, Thanks to the union bound,

$$\mathbb{P} \left( \max_{j=1, \dots, D} |\hat{T}_j - T_j| > n\delta_n \right) \leq \sum_{j=1}^D \mathbb{P} \left( |\hat{T}_j - T_j| > n\delta_n \right),$$

thus it suffices to show for each  $j = 1, \dots, D$ , that  $\mathbb{P} \left( |\hat{T}_j - T_j| > n\delta_n \right) \rightarrow 0$ . We denote by  $A_{n,j}$  the event

$$\left\{ |\hat{T}_j - T_j| > n\delta_n \right\}.$$

Similarly to Kolar and Xing (2012), we first consider the good case where we assume that the event  $C_n = \left\{ |\hat{T}_j - T_j| < \frac{\Delta_{\min}}{2} \right\}$  occurs.

### Bounding the good case

For each  $j = 1, \dots, D$ , we are going to show that  $\mathbb{P}(A_{n,j} \cap C_n) \rightarrow 0$ . In particular, we suppose that  $\hat{T}_j \leq T_j$  as the proof for  $\hat{T}_j \geq T_j$  will be the same by symmetry. Applying Lemma 1 with  $k = \hat{T}_j$  and  $k = T_j$ , subtracting one with the other and applying the  $\ell_2$ -norm, we obtain:

$$\begin{aligned} 0 &= \left\| \sum_{i=\hat{T}_j}^{T_j-1} x_{\lambda_a}^{(i)} \left\{ \tanh\left(\hat{\beta}^{(i)T} x_{\lambda_a}^{(i)}\right) - \tanh\left(\omega_a^{(i)T} x_{\lambda_a}^{(i)}\right) \right\} \right. \\ &\quad \left. - \sum_{i=\hat{T}_j}^{T_j-1} x_{\lambda_a}^{(i)} \left\{ x_a^{(i)} - \mathbb{E}_{\Omega^{(i)}} \left[ X_a | X_{\lambda_a} = x_{\lambda_a}^{(i)} \right] \right\} \right. \\ &\quad \left. + \lambda_1 (\hat{\mathbf{z}}_{\hat{T}_j} - \hat{\mathbf{z}}_{T_j}) + \lambda_2 \sum_{i=\hat{T}_j}^{T_j-1} \hat{\mathbf{y}}_i \right\|_2 \\ &\geq \left\| \sum_{i=\hat{T}_j}^{T_j-1} x_{\lambda_a}^{(i)} \left\{ \tanh\left(\hat{\beta}^{(i)T} x_{\lambda_a}^{(i)}\right) - \tanh\left(\omega_a^{(i)T} x_{\lambda_a}^{(i)}\right) \right\} \right. \\ &\quad \left. - \sum_{i=\hat{T}_j}^{T_j-1} x_{\lambda_a}^{(i)} \left\{ x_a^{(i)} - \mathbb{E}_{\Omega^{(i)}} \left[ X_a | X_{\lambda_a} = x_{\lambda_a}^{(i)} \right] \right\} \right\|_2 \\ &\quad - \left\| \lambda_2 \sum_{i=\hat{T}_j}^{T_j-1} \hat{\mathbf{y}}_i \right\|_2 - \left\| \lambda_1 (\hat{\mathbf{z}}_{\hat{T}_j} - \hat{\mathbf{z}}_{T_j}) \right\|_2. \end{aligned}$$

We have  $\left\| \lambda_1 (\hat{\mathbf{z}}_{\hat{T}_j} - \hat{\mathbf{z}}_{T_j}) \right\|_2 \leq 2\lambda_1$  and  $\left\| \lambda_2 \sum_{i=\hat{T}_j}^{T_j-1} \hat{\mathbf{y}}_i \right\|_2 \leq (T_j - \hat{T}_j) \sqrt{p-1} \lambda_2$ . Furthermore, one may notice that for all  $i \in \{\hat{T}_j, \dots, T_j - 1\}$ ,  $\hat{\beta}^{(i)} = \hat{\theta}_a^{j+1}$  and  $\omega_a^{(i)} = \theta_a^j$ .

Adding and subtracting  $\tanh\left((\theta_a^{j+1})^T x_{\lambda_a}^{(i)}\right)$ , then applying again the triangle inequality leads to the following result:

$$2\lambda_1 + (T_j - \hat{T}_j) \sqrt{p-1} \lambda_2 \geq \|R_1\|_2 - \|R_2\|_2 - \|R_3\|_2 \quad (4)$$

with

$$R_1 = \sum_{i=\hat{T}_j}^{T_j-1} x_{\lambda_a}^{(i)} \left\{ \tanh\left((\theta_a^j)^T x_{\lambda_a}^{(i)}\right) - \tanh\left((\theta_a^{j+1})^T x_{\lambda_a}^{(i)}\right) \right\} \quad (5)$$

$$R_2 = \sum_{i=\hat{T}_j}^{T_j-1} x_{\lambda_a}^{(i)} \left\{ \tanh\left((\hat{\theta}_a^{j+1})^T x_{\lambda_a}^{(i)}\right) - \tanh\left((\theta_a^{j+1})^T x_{\lambda_a}^{(i)}\right) \right\} \quad (6)$$

$$R_3 = \sum_{i=\hat{T}_j}^{T_j-1} x_{\lambda_a}^{(i)} \left\{ x_a^{(i)} - \mathbb{E}_{\Theta^{(j)}} \left[ X_a | X_{\lambda_a} = x_{\lambda_a}^{(i)} \right] \right\}. \quad (7)$$

The event (4) occurs with probability one and it can be showed that it is included in the event:

$$\begin{aligned} &\left\{ 2\lambda_1 + (T_j - \hat{T}_j) \sqrt{p-1} \lambda_2 \geq \frac{1}{3} \|R_1\|_2 \right\} \\ &\cup \left\{ \|R_2\|_2 \geq \frac{1}{3} \|R_1\|_2 \right\} \cup \left\{ \|R_3\|_2 \geq \frac{1}{3} \|R_1\|_2 \right\}. \end{aligned}$$

Thus, we have:

$$\begin{aligned} \mathbb{P}(A_{n,j} \cap C_n) &\leq \\ \mathbb{P}(A_{n,j} \cap C_n \cap \left\{ 2\lambda_1 + (T_j - \hat{T}_j) \sqrt{p-1} \lambda_2 \geq \frac{1}{3} \|R_1\|_2 \right\}) &+ \\ \mathbb{P}(A_{n,j} \cap C_n \cap \left\{ \|R_2\|_2 \geq \frac{1}{3} \|R_1\|_2 \right\}) &+ \\ \mathbb{P}(A_{n,j} \cap C_n \cap \left\{ \|R_3\|_2 \geq \frac{1}{3} \|R_1\|_2 \right\}) & \\ \triangleq \mathbb{P}(A_{n,j,1}) + \mathbb{P}(A_{n,j,3}) + \mathbb{P}(A_{n,j,3}). & \end{aligned}$$

We are going to show that each one of the three events has a probability that converges to 0 as  $n$  grows. Let's focus on  $A_{n,j,1}$ . Applying the mean-value theorem, we have for all  $i = \hat{T}_j, \dots, T_j - 1$ :

$$\begin{aligned} &\tanh\left((\theta_a^j)^T x_{\lambda_a}^{(i)}\right) - \tanh\left((\theta_a^{j+1})^T x_{\lambda_a}^{(i)}\right) \\ &= (1 - \tanh^2(\bar{\theta}^i)) x_{\lambda_a}^{(i)T} (\theta_a^j - \theta_a^{j+1}), \quad (8) \end{aligned}$$

with  $\bar{\theta}^i = \alpha^i \theta_a^j + (1 - \alpha^i) \theta_a^{j+1}$ , for a certain  $\alpha^i \in [0, 1]$ . Combining (8) with the definition of  $R_1$ , we obtain:

$$\begin{aligned} \|R_1\|_2 &= \left\| \sum_{i=\hat{T}_j}^{T_j-1} x_{\lambda_a}^{(i)} \left\{ \tanh\left((\theta_a^j)^T x_{\lambda_a}^{(i)}\right) - \tanh\left((\theta_a^{j+1})^T x_{\lambda_a}^{(i)}\right) \right\} \right\|_2 \\ &= (T_j - \hat{T}_j) \left\| \frac{1}{T_j - \hat{T}_j} \sum_{i=\hat{T}_j}^{T_j-1} (1 - \tanh^2(\bar{\theta}^{iT} x_{\lambda_a}^{(i)})) \times \right. \\ &\quad \left. \times x_{\lambda_a}^{(i)} x_{\lambda_a}^{(i)T} (\theta_a^j - \theta_a^{j+1}) \right\|_2 \\ &\geq (T_j - \hat{T}_j) \times \\ &\quad \times \Lambda_{\min} \left( \frac{1}{T_j - \hat{T}_j} \sum_{i=\hat{T}_j}^{T_j-1} (1 - \tanh^2(\bar{\theta}^{iT} x_{\lambda_a}^{(i)})) x_{\lambda_a}^{(i)} x_{\lambda_a}^{(i)T} \right) \end{aligned} \quad (9)$$

$$\times \|\theta_a^j - \theta_a^{j+1}\|_2. \quad (11)$$

Since,  $\forall j$ ,  $\|\theta_a^j\|_2 \leq M$ , we have  $\|\bar{\theta}^i\|_2 \leq M$  and  $|\bar{\theta}^{iT} x_{\lambda_a}^{(i)}| \leq M \cdot \sqrt{p-1}$ . Thus, there exist a constant  $\tilde{M} > 0$  such that  $1 - \tanh^2(\bar{\theta}^{iT} x_{\lambda_a}^{(i)}) \geq \tilde{M}$ . Combining this with the fact that each matrix  $x_{\lambda_a}^{(i)} x_{\lambda_a}^{(i)T}$  are positive semidefinite, we have:

$$\|R_1\|_2 \geq (T_j - \hat{T}_j) \tilde{M} \Lambda_{\min} \left( \frac{1}{T_j - \hat{T}_j} \sum_{i=\hat{T}_j}^{T_j-1} x_{\lambda_a}^{(i)} x_{\lambda_a}^{(i)T} \right) \xi_{\min}. \quad (12)$$

Thus, the event  $\{2\lambda_1 + (T_j - \hat{T}_j) \sqrt{p-1} \lambda_2 \geq \frac{1}{3} \|R_1\|_2\}$  is included in the event:

$$2\lambda_1 + (T_j - \hat{T}_j) \sqrt{p-1} \lambda_2 \geq (T_j - \hat{T}_j) \tilde{M} \Lambda_{\min} \left( \frac{1}{T_j - \hat{T}_j} \sum_{i=\hat{T}_j}^{T_j-1} x_{\lambda_a}^{(i)} x_{\lambda_a}^{(i)T} \right) \xi_{\min} \quad (13)$$

Denoting by  $\{13\}$  the upper event, we have:

$$\begin{aligned} \mathbb{P}(A_{n,j,1}) &\leq \mathbb{P}(A_{n,j} \cap C_n \cap \{13\}) \\ &\leq \mathbb{P} \left( A_{n,j} \cap C_n \cap \{13\} \right. \\ &\quad \left. \cap \left\{ \Lambda_{\min} \left( \frac{1}{T_j - \hat{T}_j} \sum_{i=\hat{T}_j}^{T_j-1} x_{\lambda_a}^{(i)} x_{\lambda_a}^{(i)T} \right) > \frac{\phi_{\min}}{2} \right\} \right) \\ &+ \mathbb{P} \left( A_{n,j} \cap C_n \right. \\ &\quad \left. \cap \left\{ \Lambda_{\min} \left( \frac{1}{T_j - \hat{T}_j} \sum_{i=\hat{T}_j}^{T_j-1} x_{\lambda_a}^{(i)} x_{\lambda_a}^{(i)T} \right) \leq \frac{\phi_{\min}}{2} \right\} \right) \end{aligned}$$

Using Lemma 3 with  $v_n = n\delta_n$  and  $\epsilon = \frac{\phi_{\min}}{2}$ , we can bound the right-hand side of the upper equation. We also re-write the first term so that we obtain:

$$\begin{aligned} \mathbb{P}(A_{n,j,1}) &\leq \mathbb{P}(A_{n,j} \cap C_n \cap \left\{ \frac{2\lambda_1}{T_j - \hat{T}_j} + \sqrt{p-1} \lambda_2 > \frac{\tilde{M} \phi_{\min}}{2} \xi_{\min} \right\}) \\ &\quad + c_1 \exp \left( -\frac{\epsilon^2 n \delta_n}{2} + 2 \log(n) \right) \\ &\leq \mathbb{P}(\xi_{\min}^{-1} \frac{2\lambda_1}{n\delta_n} + \xi_{\min}^{-1} \sqrt{p-1} \lambda_2 > \frac{\tilde{M} \phi_{\min}}{2}) \\ &\quad + c_1 \exp \left( -\frac{\epsilon^2 n \delta_n}{2} + 2 \log(n) \right). \end{aligned}$$

To have (iii) of the Theorem, we must have  $n\delta_n$  that goes to infinity faster than  $\log(n)$ , thus the second term of the sum goes to 0 as  $n$  grows. Furthermore, using (i) and (ii) we have:

$$\begin{aligned} \mathbb{P}(\xi_{\min}^{-1} \frac{2\lambda_1}{n\delta_n} + \xi_{\min}^{-1} \sqrt{p-1} \lambda_2 > \frac{\tilde{M} \phi_{\min}}{2}) \\ \xrightarrow{n \rightarrow 0} \mathbb{P}(0+0 > \frac{\tilde{M} \phi_{\min}}{2}) = 0. \end{aligned}$$

Which concludes that  $\mathbb{P}(A_{n,j,1}) \rightarrow 0$ .

We now focus on the event  $A_{n,j,2}$ . Let  $\bar{T}_j \triangleq \lfloor 2^{-1}(T_j + T_{j+1}) \rfloor$  and remark that between  $T_j$  and  $\bar{T}_j$ ,  $\hat{\beta}^{(i)} = \hat{\theta}^{j+1}$ . Now, using Lemma 1 with  $k = \bar{T}_j$  and  $k = T_j$  so as arguments that we used to show the equation (4), we have:

$$\begin{aligned} 2\lambda_1 + (T_j - \hat{T}_j) \sqrt{p-1} \lambda_2 &\geq \left\| \sum_{i=T_j}^{\bar{T}_j-1} x_{\lambda_a}^{(i)} \left( \tanh \left( (\hat{\theta}_a^{j+1})^T x_{\lambda_a}^{(i)} \right) \right. \right. \\ &\quad \left. \left. - \tanh \left( (\theta_a^{j+1})^T x_{\lambda_a}^{(i)} \right) \right) \right\|_2 \\ &+ \left\| \sum_{i=T_j}^{\bar{T}_j-1} x_{\lambda_a}^{(i)} \underbrace{\left( x_{\lambda_a}^{(i)} - \mathbb{E}_{\Theta^{(j+1)}} \left[ X_a | X_{\lambda_a} = x_{\lambda_a}^{(i)} \right] \right)}_{\varepsilon_{j+1}^i} \right\|_2. \end{aligned}$$

Now using the fact that  $\|\hat{\theta}_a^{j+1}\|_2$  is necessarily bounded, Lemma 3 with  $\epsilon = \phi_{\min}/2$  and similar arguments that we used for  $A_{n,j,1}$ , we have

$$\begin{aligned} \left\| \hat{\theta}_a^{j+1} - \theta_a^{j+1} \right\|_2 &\leq \\ \frac{8\lambda_1 + 4(\bar{T}_j - T_j) \sqrt{p-1} \lambda_2 + 4 \left\| \sum_{i=T_j}^{\bar{T}_j-1} x_{\lambda_a}^{(i)} \varepsilon_{j+1}^i \right\|_2}{C \phi_{\min} (T_{j+1} - T_j)}, & \quad (14) \end{aligned}$$

which holds with probability tending to one and with  $C$  a positive constant derived the same way as  $\tilde{M}$  in the previous part of the proof.

Furthermore, with probability also tending to one it can be shown that  $\|R_1\|_2 \geq (T_j - \hat{T}_j) \tilde{M} \phi_{\min} \xi_{\min} / 2$  and  $\|R_2\|_2 \leq \left\| \hat{\theta}_a^{j+1} - \theta_a^{j+1} \right\|_2 \phi_{\max} (T_j - \hat{T}_j) / 2$ . Combining that with equation (14), we can write:

$$\begin{aligned} \mathbb{P}(A_{n,j,2}) &\leq \mathbb{P}(A_{n,j} \cap C_n \cap \{C \tilde{M} \phi_{\min}^2 \phi_{\max}^{-1} \xi_{\min} (T_{j+1} - T_j) \\ &\leq 8\lambda_1 + 4(\bar{T}_j - T_j) \sqrt{p-1} \lambda_2 + 4 \left\| \sum_{i=T_j}^{\bar{T}_j-1} x_{\lambda_a}^{(i)} \varepsilon_{j+1}^i \right\|_2 \}) \end{aligned}$$

$$\begin{aligned}
 & + c_1 \exp(-c_2 n \delta_n + 2 \log(n)) \\
 \leq & \mathbb{P}(c_3 \phi_{\min}^2 \phi_{\max}^{-1} \xi_{\min} \Delta_{\min} \leq \lambda_1) \\
 & + \mathbb{P}(c_4 \phi_{\min}^2 \phi_{\max}^{-1} \xi_{\min} \leq \sqrt{p-1} \lambda_2) \\
 & + \mathbb{P}\left(c_5 \phi_{\min}^2 \phi_{\max}^{-1} \xi_{\min} \leq (\bar{T}_j - T_j)^{-1} \left\| \sum_{i=T_j}^{\bar{T}_j-1} x_{\sqrt{a}}^{(i)} \varepsilon_{j+1}^i \right\|_2\right) \\
 & + c_1 \exp(-c_2 n \delta_n + 2 \log(n)).
 \end{aligned}$$

With  $c_1, \dots, c_5$  positive constants.

The first two terms tends to 0 as  $n$  goes to infinity thanks to the hypothesis of the theorem. Indeed, since  $\Delta_{\min} > n \delta_n$  and  $(n \delta_n \xi_{\min})^{-1} \lambda_1 \rightarrow 0$  (i), the first term tends to  $\mathbb{P}(c_3 \phi_{\min}^2 \phi_{\max}^{-1} \xi_{\min} \leq 0) = 0$  and the second term tends to 0 since  $\xi_{\min}^{-1} \sqrt{p-1} \lambda_2 \rightarrow 0$  (ii). The fourth term directly tends to 0. Applying Lemma 4, we can upper bound the third term by:

$$\begin{aligned}
 & \mathbb{P}\left(c_5 \phi_{\min}^2 \phi_{\max}^{-1} \xi_{\min} \leq (\bar{T}_j - T_j)^{-1/2} 2 \sqrt{p \log(n)}\right) \\
 & \quad + c_6 \exp(-2p \log(n)) \\
 \leq & \mathbb{P}\left(c_5 \phi_{\min}^2 \phi_{\max}^{-1} \xi_{\min} \leq (n \delta_n)^{-1/2} 2 \sqrt{p \log(n)}\right) \\
 & \quad + c_6 \exp(-2p \log(n)).
 \end{aligned}$$

with  $c_6$  an other positive constant.

Since  $(\xi_{\min} \sqrt{n \delta_n})^{-1} \sqrt{p \log(n)} \rightarrow 0$  (iii), the previous equation tends to 0, which make  $\mathbb{P}(A_{n,j,2})$  tends to 0 as well.

Finally, we upper bound the probability on the event  $A_{n,j,3}$ . As before, we know that  $\|R_1\|_2 \geq (T_j - \hat{T}_j) \tilde{M} \phi_{\min} \xi_{\min} / 2$  with probability at least  $1 - c_1 \exp(-c_2 n \delta_n + 2 \log(n))$ , thus we have:

$$\begin{aligned}
 \mathbb{P}(A_{n,j,3}) \leq & \mathbb{P}\left(\frac{\tilde{M} \phi_{\min} \xi_{\min}}{6} \leq \frac{\|R_3\|_2}{T_j - \hat{T}_j}\right) \\
 & + c_1 \exp(-c_2 n \delta_n + 2 \log(n))
 \end{aligned}$$

Using Lemma 5, we can upper bound the first term by:

$$\begin{aligned}
 & \mathbb{P}\left(\frac{\tilde{M} \phi_{\min} \xi_{\min}}{6} \leq 2 \sqrt{\frac{p \log(n)}{T_j - \hat{T}_j}}\right) + c_2 \exp(-c_3 \log(n)) \\
 \leq & \mathbb{P}\left(\frac{\tilde{M} \phi_{\min} \xi_{\min}}{6} \leq 2 \sqrt{\frac{p \log(n)}{n \delta_n}}\right) + c_2 \exp(-c_3 \log(n))
 \end{aligned}$$

which tends to 0 thanks to (iii). Since the symmetric case follows exactly the same arguments, we have shown that  $\mathbb{P}(A_{n,j} \cap C_n) \rightarrow 0$ . We now need to prove that  $\mathbb{P}(A_{n,j} \cap C_n^c) \rightarrow 0$ .

## Bounding the bad case

Again, the proof closely follows the one of Harchaoui and Lévy-Leduc (2010); Kolar and Xing (2012); Gibberd and Roy (2017). Let define the following complementary events:

$$D_n^{(l)} \triangleq \left\{ \exists j \in [D], \hat{T}_j \leq T_{j-1} \right\} \cap C_n^c \quad (15)$$

$$D_n^{(m)} \triangleq \left\{ \forall j \in [D], T_{j-1} < \hat{T}_j < T_{j+1} \right\} \cap C_n^c \quad (16)$$

$$D_n^{(r)} \triangleq \left\{ \exists j \in [D], \hat{T}_j \geq T_{j+1} \right\} \cap C_n^c. \quad (17)$$

We can write  $\mathbb{P}(A_{n,j} \cap C_n^c) = \mathbb{P}(A_{n,j} \cap D_n^{(l)}) + \mathbb{P}(A_{n,j} \cap D_n^{(m)}) + \mathbb{P}(A_{n,j} \cap D_n^{(r)})$ . Again, the goal is to prove that the three terms tends to 0. We will assume that  $\hat{T}_j \leq T_j$  as the other case can be done by symmetry. Let's first focus on the middle term, it has been shown in Harchaoui and Lévy-Leduc (2010); Kolar and Xing (2012); Gibberd and Roy (2017) that it can be upper bounded in the following way:

$$\begin{aligned}
 & \mathbb{P}(A_{n,j} \cap D_n^{(m)}) \\
 \leq & \mathbb{P}(A_{n,j} \cap \{(\hat{T}_{j+1} - T_j) \geq \frac{\Delta_{\min}}{2}\} \cap D_n^{(m)}) \\
 & + \mathbb{P}(\{(T_{j+1} - \hat{T}_{j+1}) \geq \frac{\Delta_{\min}}{2}\} \cap D_n^{(m)}) \\
 \leq & \mathbb{P}(A_{n,j} \cap \{(\hat{T}_{j+1} - T_j) \geq \frac{\Delta_{\min}}{2}\} \cap D_n^{(m)}) \\
 & + \sum_{k=j+1}^D \mathbb{P}(\{(\hat{T}_{k+1} - T_k) \geq \frac{\Delta_{\min}}{2}\} \\
 & \quad \cap \{(T_k - \hat{T}_k) \geq \frac{\Delta_{\min}}{2}\} \cap D_n^{(m)}). \quad (18)
 \end{aligned}$$

Let's bound the first term. Assuming the event  $A_{n,j} \cap \{(\hat{T}_{j+1} - T_j) \geq \frac{\Delta_{\min}}{2}\} \cap D_n^{(m)}$  and applying Lemma 1 with  $k = \hat{T}_j$  and  $k = T_j$ , we can prove similarly as equation (14) that:

$$\begin{aligned}
 & \left\| \hat{\theta}_a^{j+1} - \theta_a^j \right\|_2 \\
 \leq & \frac{4\lambda_1 + 2(T_j - \hat{T}_j) \sqrt{p-1} \lambda_2 + 2 \left\| \sum_{i=\hat{T}_j}^{T_j-1} x_{\sqrt{a}}^{(i)} \varepsilon_j^i \right\|_2}{C \phi_{\min}(T_j - \hat{T}_j)} \\
 \leq & c_1 \phi_{\min}^{-1} (n \delta_n)^{-1} \lambda_1 + c_2 \phi_{\min}^{-1} \sqrt{p-1} \lambda_2 \\
 & + c_3 \phi_{\min}^{-1} (T_j - \hat{T}_j)^{-1} \left\| \sum_{i=\hat{T}_j}^{T_j-1} x_{\sqrt{a}}^{(i)} \varepsilon_j^i \right\|_2.
 \end{aligned}$$

with probability tending to one. Using Lemma 5 we can bound the third term and obtain:

$$\left\| \hat{\theta}_a^{j+1} - \theta_a^j \right\|_2 \leq c_1 \phi_{\min}^{-1} (n \delta_n)^{-1} \lambda_1 + c_2 \phi_{\min}^{-1} \sqrt{p-1} \lambda_2$$

$$+ c_3 \phi_{\min}^{-1} (\sqrt{n\delta_n})^{-1} \sqrt{p \log(n)}$$

with probability tending to one. Similarly, applying the same lemmas with  $k = T_j$  and either  $k = \widehat{T}_{j+1}$ , if  $\widehat{T}_{j+1} \leq T_{j+1}$  or  $k = T_{j+1}$  otherwise, we have:

$$\begin{aligned} \left\| \widehat{\theta}_a^{j+1} - \theta_a^{j+1} \right\|_2 &\leq c_4 \phi_{\min}^{-1} (n\delta_n)^{-1} \lambda_1 + c_5 \phi_{\min}^{-1} \sqrt{p-1} \lambda_2 \\ &\quad + c_6 \phi_{\min}^{-1} (\sqrt{n\delta_n})^{-1} \sqrt{p \log(n)} \end{aligned}$$

with probability tending to one.

Since  $\xi_{\min} \leq \left\| \theta_a^j - \theta_a^{j+1} \right\|_2 \leq \left\| \widehat{\theta}_a^{j+1} - \theta_a^j \right\|_2 + \left\| \widehat{\theta}_a^{j+1} - \theta_a^{j+1} \right\|_2$ , we finally upper bound the considered probability by:

$$\begin{aligned} &\mathbb{P}(A_{n,j} \cap \{(\widehat{T}_{j+1} - T_j) \geq \frac{\Delta_{\min}}{2}\} \cap D_n^{(m)}) \\ &\leq \mathbb{P}(\xi_{\min} \leq c_7 \phi_{\min}^{-1} (n\delta_n)^{-1} \lambda_1 + c_8 \phi_{\min}^{-1} \sqrt{p-1} \lambda_2 \\ &\quad + c_9 \phi_{\min}^{-1} (\sqrt{n\delta_n})^{-1} \sqrt{p \log(n)}). \end{aligned}$$

Which tends to 0 thanks to the hypothesis (i), (ii) and (iii). The other probabilities in the upper bound on  $\mathbb{P}(A_{n,j} \cap D_n^{(m)})$  also tends to 0. The proof follows exactly the previous one. We proved that  $\mathbb{P}(A_{n,j} \cap D_n^{(m)}) \rightarrow 0$ , we will now show the same for  $\mathbb{P}(A_{n,j} \cap D_n^{(l)})$ .

The proof exactly follows the one of Gibberd and Roy (2017) where it has been showed that:

$$\begin{aligned} \mathbb{P}(D_n^{(l)}) &\leq \sum_{j=1}^D 2^{j-1} \mathbb{P}(\max\{l \in [D] : \widehat{T}_l \leq T_{l-1}\}) \\ &\leq 2^{D-1} \sum_{j=1}^D \sum_{l>j} \mathbb{P}(\{T_l - \widehat{T}_l \geq \frac{\Delta_{\min}}{2}\} \\ &\quad \cap \{\widehat{T}_{l+1} - T_l \geq \frac{\Delta_{\min}}{2}\}). \end{aligned}$$

Now, as shown in Gibberd and Roy (2017) and with the same arguments used to bound the elements of (18), we have  $\mathbb{P}(D_n^{(l)}) \rightarrow 0$ . Similarly we can show  $\mathbb{P}(D_n^{(r)}) \rightarrow 0$  as  $n \rightarrow 0$ . Finally we have  $\mathbb{P}(A_{n,j} \cap C_n^c) \rightarrow 0$ , which concludes the proof.  $\square$

**Lemma 2.** *Let  $\{x^{(i)}\}_{i=1}^n$  be a set of i.i.d observation sampled from an Ising model with parameter  $\Theta \in \mathbb{R}^{p \times p}$  and assume that assumption (A1) is satisfied. Then,  $\forall r, l \in [n]$  such that  $l < r$  and  $r-l > v_n$  with  $v_n$  a positive series, we have  $\forall \epsilon > 0$ :*

$$\begin{aligned} \mathbb{P}\left(\Lambda_{\min}\left(\frac{1}{r-l+1} \sum_{i=l}^r x_{\lambda_a}^{(i)} x_{\lambda_a}^{(i)T}\right) \leq \phi_{\min} - \epsilon\right) \\ \leq 2(p-1)^2 \exp\left(-\frac{\epsilon^2 v_n}{2}\right) \end{aligned} \quad (19)$$

and

$$\begin{aligned} \mathbb{P}\left(\Lambda_{\max}\left(\frac{1}{r-l+1} \sum_{i=l}^r x_{\lambda_a}^{(i)} x_{\lambda_a}^{(i)T}\right) \geq \phi_{\max} + \epsilon\right) \\ \leq 2(p-1)^2 \exp\left(-\frac{\epsilon^2 v_n}{2}\right) \end{aligned} \quad (20)$$

*Proof.* Let  $\widehat{\Sigma} = \frac{1}{r-l+1} \sum_{i=l}^r x_{\lambda_a}^{(i)} x_{\lambda_a}^{(i)T}$  and  $\Sigma = \mathbb{E}[X_{\lambda_a} X_{\lambda_a}^T]$ .

We first proof inequality (19). Recall that for a symmetric matrix  $M$ , we have  $\Lambda_{\max}(M) \leq \|M\|_F$ , the Frobenius norm of  $M$ . We have

$$\Lambda_{\min}(\widehat{\Sigma}) = \min_{\|v\|_2=1} v^T \widehat{\Sigma} v \quad (21)$$

$$\geq \min_{\|v\|_2=1} v^T \Sigma v - \max_{\|v\|_2=1} v^T (\widehat{\Sigma} - \Sigma) v \quad (22)$$

$$\geq \Lambda_{\min}(\Sigma) - \Lambda_{\max}(\widehat{\Sigma} - \Sigma) \quad (23)$$

$$\geq \phi_{\min} - \left\| \widehat{\Sigma} - \Sigma \right\|_F. \quad (24)$$

Let  $s_{mq}^{(i)}$  be the  $(m, q)$ -th coordinate of  $x_{\lambda_a}^{(i)} x_{\lambda_a}^{(i)T} - \Sigma$  and  $\frac{1}{r-l+1} \sum_{i=l}^r s_{mq}^{(i)}$  the one of  $\widehat{\Sigma} - \Sigma$ . Note that  $\mathbb{E}[s_{mq}^{(i)}] = 0$  and  $|s_{mq}^{(i)}| \leq 2$ . Let's analyze the quantity  $\mathbb{P}\left(\left\| \widehat{\Sigma} - \Sigma \right\|_F > \epsilon\right)$  with  $\epsilon > 0$ :

$$\mathbb{P}\left(\left\| \widehat{\Sigma} - \Sigma \right\|_F > \epsilon\right) = \mathbb{P}\left(\left(\sum_{m,q} s_{mq}^2\right)^{1/2} > \epsilon\right) \quad (25)$$

$$= \mathbb{P}\left(\sum_{m,q} s_{mq}^2 > \epsilon^2\right) \quad (26)$$

$$\leq \sum_{m,q} \mathbb{P}(s_{mq}^2 > \epsilon^2) \quad (27)$$

$$\leq \sum_{m,q} \mathbb{P}(|s_{mq}| > \epsilon). \quad (28)$$

Thanks to Hoeffding's inequality, we have  $\mathbb{P}(|s_{mq}| > \epsilon) \leq 2 \exp\left(-\frac{\epsilon^2 (r-l+1)}{2}\right)$ . Since  $r-l > v_n$ , we also have  $\mathbb{P}(|s_{mq}| > \epsilon) \leq 2 \exp\left(-\frac{\epsilon^2 v_n}{2}\right)$ . It follows from (28) that  $\mathbb{P}\left(\left\| \widehat{\Sigma} - \Sigma \right\|_F > \epsilon\right) \leq 2(p-1)^2 \exp\left(-\frac{\epsilon^2 v_n}{2}\right)$ . We deduce that:

$$\mathbb{P}\left(\Lambda_{\min}(\widehat{\Sigma}) \geq \phi_{\min} - \epsilon\right) \geq 1 - 2(p-1)^2 \exp\left(-\frac{\epsilon^2 v_n}{2}\right), \quad (29)$$

which concludes the proof for (19).

To prove (20) it suffices to note that  $\Lambda_{\max}(\widehat{\Sigma}) \leq \phi_{\max} + \left\| \widehat{\Sigma} - \Sigma \right\|_F$  and use the same arguments.  $\square$

**Lemma 3.** Let  $\{x^{(i)}\}_{i=1}^n$  be a set of i.i.d observation sampled from an Ising model with parameter  $\Theta \in \mathbb{R}^{p \times p}$  and assume that assumption **(A1)** is satisfied.

Let  $R$  and  $L$  be two random variable such that  $R, L \in [n]$ ,  $L < R$  and  $R - L > v_n$  almost surely, with  $v_n$  a positive series. For a fixed node  $a$  and any  $\epsilon > 0$ , there exist a constant  $c_1 > 0$  such that:

$$\begin{aligned} \mathbb{P} \left( \Lambda_{\min} \left( \frac{1}{R-L+1} \sum_{i=L}^R x_{\setminus a}^{(i)} x_{\setminus a}^{(i)T} \right) \leq \phi_{\min} - \epsilon \right) \\ \leq c_1 \exp \left( -\frac{\epsilon^2 v_n}{2} + 2 \log(n) \right) \end{aligned} \quad (30)$$

and

$$\begin{aligned} \mathbb{P} \left( \Lambda_{\max} \left( \frac{1}{R-L+1} \sum_{i=L}^R x_{\setminus a}^{(i)} x_{\setminus a}^{(i)T} \right) \geq \phi_{\max} + \epsilon \right) \\ \leq c_1 \exp \left( -\frac{\epsilon^2 v_n}{2} + 2 \log(n) \right). \end{aligned} \quad (31)$$

*Proof.* We note  $\widehat{\Sigma}(L, R) = \frac{1}{R-L+1} \sum_{i=L}^R x_{\setminus a}^{(i)} x_{\setminus a}^{(i)T}$  and  $\mathcal{I} \triangleq \{(l, r) \in [n]^2 : r - l > v_n\}$

We first prove inequality (30):

$$\mathbb{P} \left( \Lambda_{\max} \left( \widehat{\Sigma}(L, R) \right) \geq \phi_{\max} + \epsilon \right) \quad (32)$$

$$= \sum_{(l, r) \in \mathcal{I}} \mathbb{P} \left( \Lambda_{\max} \left( \widehat{\Sigma}(L, R) \right), L = l, R = r \right) \quad (33)$$

$$\leq \sum_{(l, r) \in \mathcal{I}} \mathbb{P} \left( \Lambda_{\max} \left( \widehat{\Sigma}(L, R) \right) \middle| L = l, R = r \right). \quad (34)$$

Using lemma 2 we can bound (34):

$$(34) \leq \sum_{(l, r) \in \mathcal{I}} 2(p-1)^2 \exp \left( -\frac{\epsilon^2 v_n}{2} \right) \quad (35)$$

$$\leq |\mathcal{I}| c_1 \exp \left( -\frac{\epsilon^2 v_n}{2} \right) \quad (36)$$

$$\leq n^2 c_1 \exp \left( -\frac{\epsilon^2 v_n}{2} \right) \quad (37)$$

$$\leq c_1 \exp \left( -\frac{\epsilon^2 v_n}{2} + 2 \log(n) \right) \quad (38)$$

with  $c_1 = 2(p-1)$ . This concludes the proof for (30). Same arguments are used to prove (31).  $\square$

**Lemma 4.** Let  $\{x^{(i)}\}_{i=1}^n$  be a set of independent observation sampled from the time-varying Ising model (Section 2). Then,  $\forall j \in [D]$  and  $\forall r, l \in \{T_j, \dots, T_{j+1}-1\}$  such that  $l < r$ , we have:

$$\mathbb{P} \left( \frac{1}{r-l+1} \|R_3(l, r)\|_2 \leq 2\sqrt{\frac{p \log(n)}{r-l+1}} \right) \quad (39)$$

$$\geq 1 - 2(p-1) \exp(-2p \log(n)) \quad (40)$$

with  $R_3(l, r) = \sum_{i=l}^r x_{\setminus a}^{(i)} \left\{ x_a^{(i)} - \mathbb{E}_{\Theta^j} [X_a | X_{\setminus a} = x_{\setminus a}^{(i)}] \right\}$ .

*Proof.* Let  $Z_{ij}$  be the the  $j$ -th element of the vector  $\frac{1}{r-l+1} x_{\setminus a}^{(i)} \left\{ x_a^{(i)} - \mathbb{E}_{\Theta} [X_a | X_{\setminus a} = x_{\setminus a}^{(i)}] \right\}$ . Note that  $|Z_{ij}| \leq \frac{2}{r-l+1}$  and  $\mathbb{E}[Z_{ij}] = 0$ . Let  $\epsilon > 0$ , we have:

$$\begin{aligned} \mathbb{P} \left( \frac{1}{r-l+1} \|R_3(l, r)\|_2 \geq \epsilon \right) \\ = \mathbb{P} \left( \sqrt{\sum_{j \neq a} \left( \sum_{i=l}^r Z_{ij} \right)^2} \geq \epsilon \right) \\ = \mathbb{P} \left( \sum_{j \neq a} \left( \sum_{i=l}^r Z_{ij} \right)^2 \geq \epsilon^2 \right) \\ \leq \sum_{j \neq a} \mathbb{P} \left( \left| \sum_{i=l}^r Z_{ij} \right| \geq \epsilon \right) \\ \leq 2(p-1) \exp \left( -\frac{\epsilon^2 (r-l+1)}{2} \right). \end{aligned}$$

Now, if we fix  $\epsilon = 2\sqrt{\frac{p \log(n)}{r-l+1}}$ , we obtain:

$$\begin{aligned} \mathbb{P} \left( \frac{1}{r-l+1} \|R_3(l, r)\|_2 \leq 2\sqrt{\frac{p \log(n)}{r-l+1}} \right) \\ \geq 1 - 2(p-1) \exp(-2p \log(n)). \end{aligned}$$

$\square$

**Lemma 5.** Let  $\{x^{(i)}\}_{i=1}^n$  be a set of independent observation sampled from the time-varying Ising model (Section 2). We have:

$$\begin{aligned} \mathbb{P} \left( \bigcap_{j \in [D]} \bigcap_{l, r \in \mathcal{I}_j} \left\{ \frac{1}{r-l+1} \|R_3^j(l, r)\|_2 \leq 2\sqrt{\frac{p \log(n)}{r-l+1}} \right\} \right) \\ \geq 1 - c_2 \exp(-c_3 \log(n)) \end{aligned} \quad (41)$$

with  $R_3^j(l, r) = \sum_{i=l}^r x_{\setminus a}^{(i)} \left\{ x_a^{(i)} - \mathbb{E}_{\Theta^j} [X_a | X_{\setminus a} = x_{\setminus a}^{(i)}] \right\}$ ,  $c_2, c_3$  some positive constants and  $\mathcal{I}_j \triangleq \{(l, r) \in \{T_j, \dots, T_{j+1}-1\}^2 : r > l\}$ .

*Proof.* The proof is a simple application of Lemma 4:

$$\begin{aligned} \mathbb{P} \left( \bigcup_{j \in [D]} \bigcup_{l, r \in \mathcal{I}_j} \left\{ \frac{1}{r-l+1} \|R_3^j(l, r)\|_2 \geq 2\sqrt{\frac{p \log(n)}{r-l+1}} \right\} \right) \\ \leq \sum_{j \in [D]} \sum_{l, r \in \mathcal{I}_j} \mathbb{P} \left( \frac{1}{r-l+1} \|R_3^j(l, r)\|_2 \geq 2\sqrt{\frac{p \log(n)}{r-l+1}} \right) \end{aligned}$$

---

$$\begin{aligned} &\leq 2Dn^2(p-1)\exp(-2p\log(n)) \\ &\leq c_2\exp(-2p\log(n)+2\log(n)) \\ &\leq c_2\exp(-c_3\log(n)), \end{aligned}$$

since  $p > 1$ . This concludes the proof.  $\square$

## References

- Gibberd, A. J. and Roy, S. (2017). Multiple changepoint estimation in high-dimensional Gaussian graphical models. *arXiv preprint arXiv:1712.05786*.
- Harchaoui, Z. and Lévy-Leduc, C. (2010). Multiple changepoint estimation with a total variation penalty. *J. of the American Statistical Association*, 105(492):1480–1493.
- Kolar, M. and Xing, E. P. (2012). Estimating networks with jumps. *Electronic Journal of Statistics*, 6:2069.



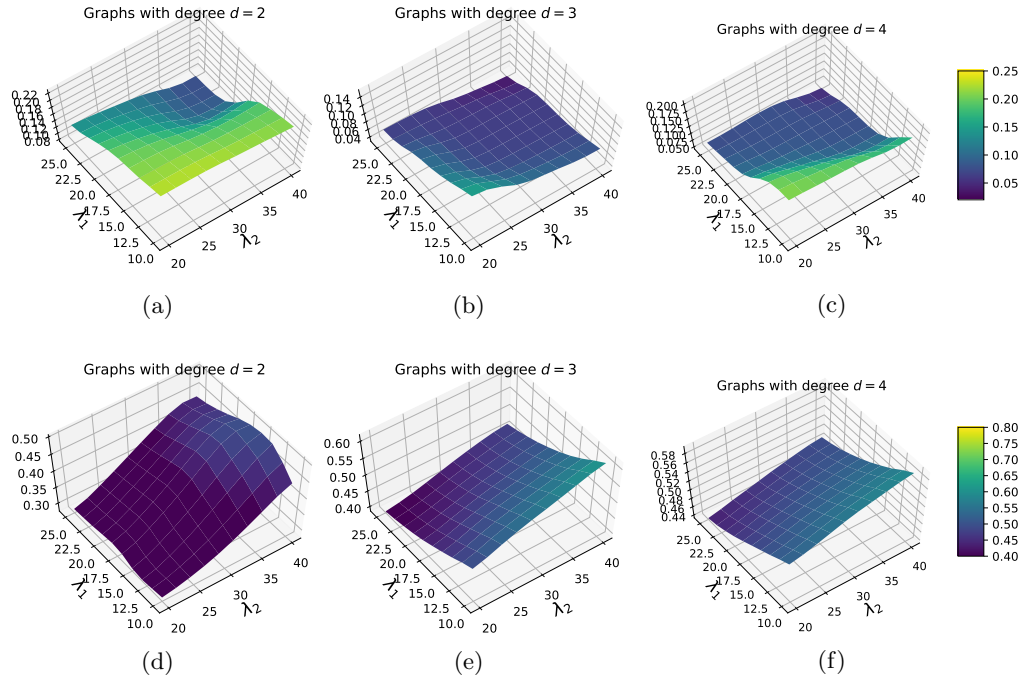


Figure 1: Heat-maps of the average  $h$ -score (a)(b)(c) and  $F_1$ -score (b)(e)(f) obtained with TD-Lasso when the degree of each node  $d$  is equal to 2, 3, or 4.

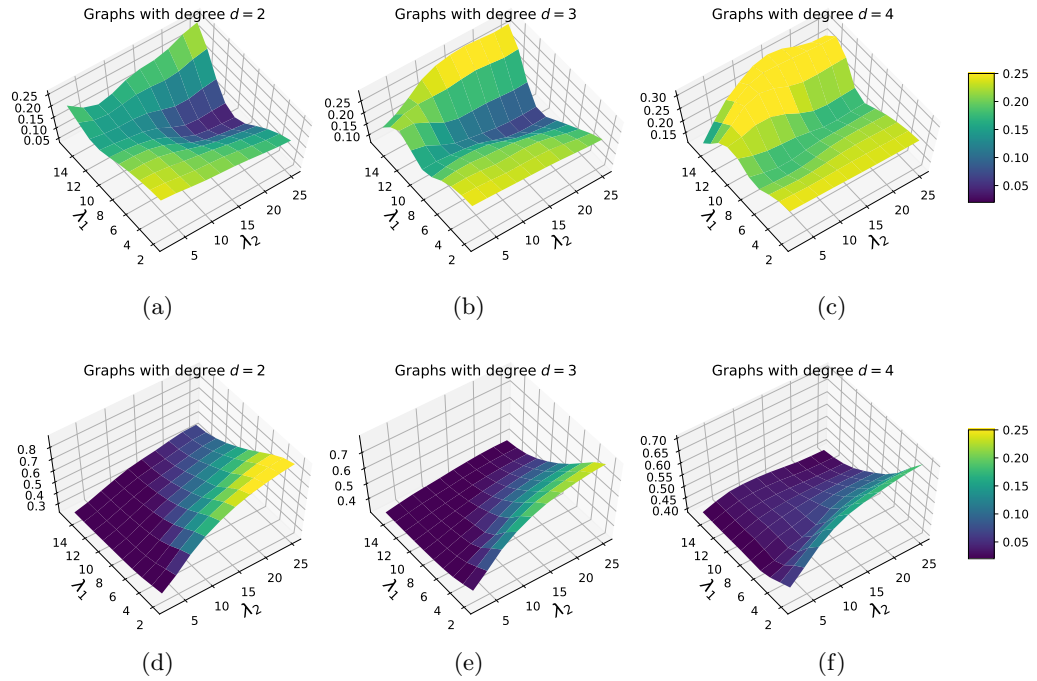


Figure 2: Heat-maps of the average  $h$ -score (a)(b)(c) and  $F_1$ -score (b)(e)(f) obtained with Tesla when the degree of each node  $d$  is equal to 2, 3, or 4.

---

	Metrics	Precision	Recall	F-measure	h-score $\leq 0.03$
$d=2$	<b>TVI-FL</b>	<b>0.613</b> $\pm 0.118$	<b>0.931</b> $\pm 0.070$	<b>0.735</b> $\pm 0.104$	0.020 $\pm 0.008$
	Tesla	0.596 $\pm 0.076$	0.792 $\pm 0.125$	0.679 $\pm 0.092$	0.017 $\pm 0.009$
	TD-lasso*	0.354	<b>0.978</b>	0.518	0.027
$d=3$	<b>TVI-FL</b>	<b>0.583</b> $\pm 0.107$	<b>0.831</b> $\pm 0.082$	<b>0.682</b> $\pm 0.094$	0.020 $\pm 0.008$
	Tesla	0.400 $\pm 0.076$	0.619 $\pm 0.060$	0.478 $\pm 0.058$	0.018 $\pm 0.007$
	TD-lasso*	0.374	<b>0.950</b>	0.536	0.027
$d=4$	<b>TVI-FL</b>	<b>0.495</b> $\pm 0.080$	<b>0.692</b> $\pm 0.068$	<b>0.575</b> $\pm 0.070$	0.024 $\pm 0.005$
	Tesla	0.332 $\pm 0.060$	0.653 $\pm 0.154$	0.424 $\pm 0.027$	0.013 $\pm 0.006$
	TD-lasso*	0.377	<b>0.870</b>	0.523	0.027
$d=5$	<b>TVI-FL</b>	<b>0.428</b> $\pm 0.083$	<b>0.648</b> $\pm 0.089$	<b>0.509</b> $\pm 0.071$	0.021 $\pm 0.009$
	Tesla	0.368 $\pm 0.079$	0.635 $\pm 0.170$	0.443 $\pm 0.022$	0.021 $\pm 0.008$
	TD-lasso*	0.367	<b>0.793</b>	0.501	0.010

Table 1: Average value and standard error of the maximum  $F_1$ -score when the  $h$ -score is lower than 0.03. \* For TD-lasso, only a maximum of 3 experiments are reaching the condition  $h\text{-score} \leq 0.03$ . Hence, we do not provide the standard deviations.